Open boundaries in a cellular automata model for synchronized flow: Effects of nonmonotonicity

Rui Jiang and Qing-Song Wu*
School of Engineering Science, University of Science and Technology of China, Hefei 230026, People's Republic of China
(Received 15 April 2003; published 29 August 2003)

In this paper, we have discussed the traffic situations arising from the open boundary conditions (OBC) of a cellular automata model that can reproduce the synchronized flow. The model is different from the slow-to-start (STS) model in that the upper branch of the fundamental diagram in the periodic boundary conditions (PBC) is not monotonous but has an extremum. The phase diagram and the fundamental diagram of the model in the OBC are investigated. The results are compared with those of the STS model and those in the PBC. The current in the OBC as well as the density profiles in the different phases is also investigated.

DOI: 10.1103/PhysRevE.68.026135 PACS number(s): 89.40.−a, 45.70.Vn, 05.40.−a, 02.60.Cb

I. INTRODUCTION

In the past few decades, traffic problems have attracted the interest of a community of physicists [1–3]. Traffic flow, a kind of many-body systems of strongly interacting vehicles, shows various complex behaviors. To understand the behavior of traffic flow, various traffic flow models have been proposed and studied, including car-following models, cellular automaton (CA) models, gas-kinetic models, and hydrodynamic models [4–12]. Compared with other dynamical approaches, CA models are conceptually simpler, and can be easily implemented on computers for numerical investigations.

The most simple CA model for traffic flow is the rule-184 CA named by Wolfram [13]. In 1992, Nagel and Schreckenberg proposed the well-known Nagel-Schreckenberg (NS) model [5]. As an extension of rule-184 CA, velocities $v_{max} > 1$ are allowed in the NS model. The NS model can reproduce some basic phenomena encountered in real traffic. However, it cannot explain all experimental results. Therefore, several improved versions of the NS model were proposed, such as the slow-to-start (STS) models [6], etc.

The CA models for traffic flow were extensively studied within periodic boundary conditions (PBC). However, open boundaries are relevant for many realistic situations in traffic. Recent researches point out that for models with a unique flow-density relation, a phenomenological theory can be developed to predict the phase diagram in the case of open boundary conditions (OBC) [14], which is similar to the one of the asymmetric simple exclusion process (ASEP).[1]

Due to the introduction of the STS rules, the STS models exhibit the metastable states and the hysteresis in the PBC. Thus, the phase diagram of these models in the OBC cannot be predicted by the phenomenological theory. Recently, this issue has been studied [17,18], and it is shown that there exist the high flow states in a certain parameter regime for finite system. Moreover, a striped structure in the high density phase is observed.

Very recently, the authors presented a new CA model which can describe the synchronized flow quite satisfactorily [19]. This model also exhibits the metastable states and the hysteresis in the PBC. Nevertheless, different from the STS model, the upper branch of the fundamental diagram of the new model is not monotonous but has an extremum. Therefore, it is interesting to analyze what additional effects can be observed due to the nonmonotonicity in the OBC.

This paper is organized as follows. In Sec. II, the model is briefly reviewed and the OBC is defined. In Secs. III and IV, the numerical simulations are carried out and the results are compared with that of STS models. The conclusions are given in Sec. V.

II. MODEL AND OPEN BOUNDARY CONDITIONS

For the sake of the completeness, we will now briefly recall the new model proposed by the authors. The model is defined by modifing the brake light rule and the STS rule of the comfortable driving (CD) model presented by Knospe *et al.* [20], thus it is referred to as modified CD (MCD) model. The parallel update rules of the MCD model are as follows.

(1) Determination of the randomization parameter p:

$$p = p(v_n(t), b_{n+1}(t), t_h, t_s).$$

(2) Acceleration:

if $[b_{n+1}(t)=0$ or $t_h \geqslant t_s]$,
and $[v_n(t)>0]$, then $v_n(t+1)=\min(v_n(t)+2, v_{max})$
else if $(v_n(t)=0)$, then $v_n(t+1)=\min(v_n(t)+1, v_{max})$
else $v_n(t+1)=v_n(t)$.

(3) Braking rule:

$$v_n(t+1)=\min(d_n^{eff}, v_n(t+1)).$$

(4) Randomization and braking:

if $[N_{\mathrm{rand}}()<p]$, then $v_n(t+1)=\max(v_n(t+1)-1, 0)$.

(5) The determination of $b_n(t+1)$:

*Corresponding author. Email address: qswu@ustc.edu.cn

[1]Cheybany *et al.* [15] and Huang [16] found large deviations in the phase diagram of the NS model in the OBC in comparison to the ASEP, which is due to the special boundary conditions used, as pointed out by Barlovic *et al.* [17].

$$\text{if } [v_n(t+1)<v_n(t)], \text{ then } b_n(t+1)=1$$

$$\text{if } [v_n(t+1)>v_n(t)], \text{ then } b_n(t+1)=0$$

$$\text{if } [v_n(t+1)=v_n(t)], \text{ then } b_n(t+1)=b_n(t).$$

(6) The determination of $t_{st,n}$:

$$\text{if } v_n(t+1)=0, \text{ then } t_{st,n}=t_{st,n}+1$$

$$\text{if } v_n(t+1)>0, \text{ then } t_{st,n}=0.$$

(7) Car motion:

$$x_n(t+1)=x_n(t)+v_n(t+1).$$

Here x_n and v_n are the position and velocity of vehicle n (here vehicle $n+1$ precedes vehicle n), d_n is the gap of the vehicle n, b_n is the status of the brake light [on(off)$\rightarrow b_n=1(0)$]. The two times $t_h=d_n/v_n(t)$ and $t_s=\min(v_n(t),h)$, where h determines the range of interaction with the brake light, are introduced to compare the time t_h needed to reach the position of the leading vehicle with a velocity-dependent interaction horizon t_s. $d_n^{eff}=d_n+\max(v_{anti}-d_{safety},0)$ is the effective distance, where $v_{anti}=\min(d_{n+1},v_{n+1})$ is the expected velocity of the preceding vehicle in the next time step and d_{safety} controls the effectiveness of the anticipation. N_{rand} is a random number between 0 and 1, $t_{st,n}$ denotes the time when the car n stops. The randomization parameter p is defined as

$$p(v_n(t),b_{n+1}(t),t_h,t_s)=\begin{cases} p_b & \text{if } b_{n+1}=1 \text{ and } t_h<t_s \\ p_0 & \text{if } v_n=0 \text{ and } t_{st,n}\geqslant t_c \\ p_d & \text{in all other cases.} \end{cases}$$

We note that in the model, (i) the acceleration capacity of a stopped car is assumed to be 1 and that of a moving car is 2; (ii) the brake light is switched on if the speed decreases, and after it is switched on, the brake light will not switch off unless the car begins to accelerate; (iii) only when the car has stopped for a certain time t_c does the driver become less sensitive.

The fundamental diagram of the model in the PBC is shown in Fig. 1, where the parameter values are $t_c=10$, $v_{max}=20$, $p_d=0.1$, $p_b=0.94$, $p_0=0.5$, $h=6$, $d_{safety}=7$.[2] Each cell corresponds to 1.5 m and a vehicle has a length of five cells. One time step corresponds to 1 s. The system size is $L=10\,000$. The density can be divided into three different regimes. When the density is low ($k<k_{c1}$), no jams appear. When density is high ($k>k_{c2}$), the system is characterized by the phase separation. Between the two densities k_{c1} and k_{c2}, the system is metastable: the homogeneous traffic will evolve into the synchronized flow; in contrast, if we start from a megajam, the phase separation occurs.

[2]Note the difference of flux between Ref. [19] and this paper. In Ref. [19], the density $k=1$ corresponds to one vehicle/five cells. Thus, the value of the flux in this paper is 0.2 times that in Ref. [19].

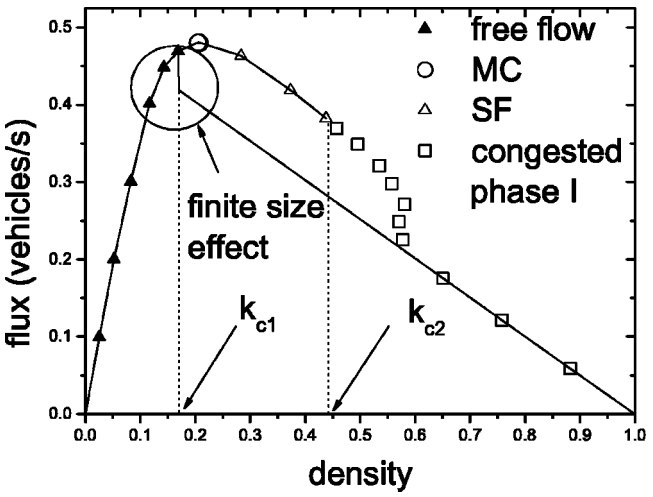

FIG. 1. The fundamental diagram of the MCD model in both PBC (solid line) and OBC (scatter points). The peak of the line is a finite size effect.

The open boundary conditions are applied as follows. We assume that the leftmost cell on the road corresponds to $x=1$, and the entrance section of the road includes v_{max} cells. In one time step, when the update of the cars on the road is completed, we check the position of the last car on the road, which is denoted as x_{last}. If $x_{last}>v_{max}$, a car with velocity v_{max} is injected with probability α at the cell $\min[x_{last}-v_{max},v_{max}]$.

The right boundary is realized by five cells linked to the end of the system. The leading car with the position x_{lead} is removed if $x_{lead}>L$ (L denotes the position of the rightmost cell on the road), and the following car becomes the new leading car. Then a random number $N'_{\text{rand}}()$ is generated: if $N'_{\text{rand}}()\geqslant\beta$, then the new leading car moves without any hindrance; otherwise the new leading car moves as if the cells $L+1,\ldots,L+5$ are occupied by a stopped car.

III. PHASE DIAGRAM AND CURRENT

In this section, the numerical simulations are carried out and the phase diagram and the current in the OBC are ana-

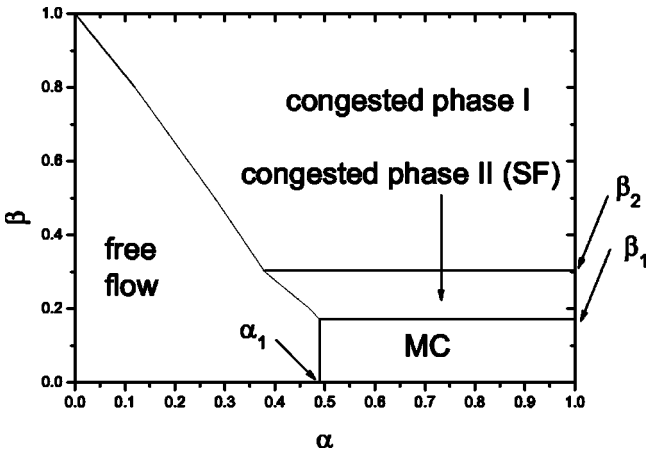

FIG. 2. The phase diagram of the MCD model in the OBC.

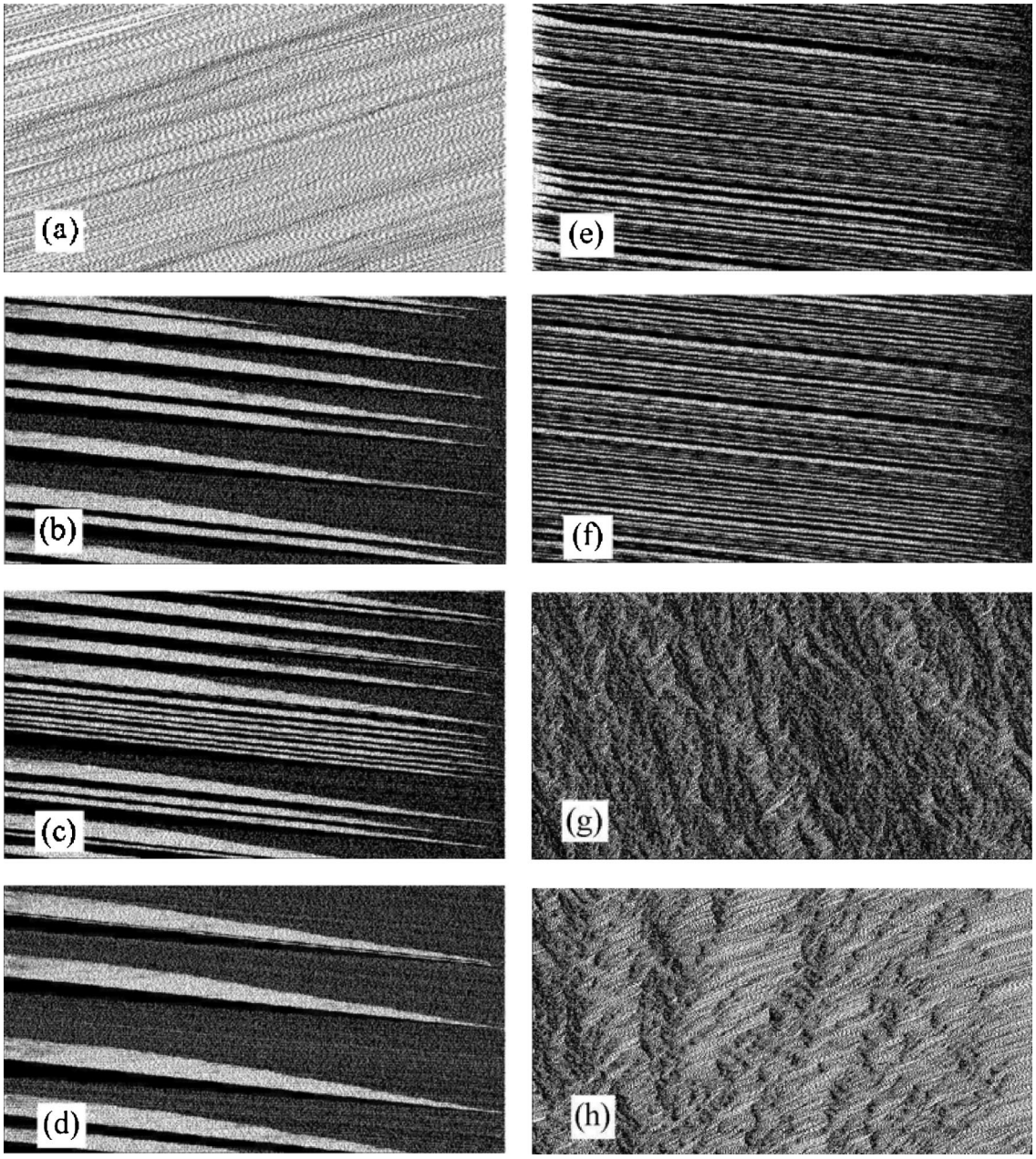

FIG. 3. The space-time plots of the model in the OBC. The cars are moving from the left to the right, and the vertical direction (up) is (increasing) time. The vertical direction corresponds to 20 000 time steps in (b)–(f) while it is 1000 time steps in other plots. (a) $\alpha=0.3,\beta=0.2$; (b) $\alpha=0.5,\beta=0.55$; (c) $\alpha=0.5,\beta=0.6$; (d) $\alpha=0.5,\beta=0.5$; (e) $\alpha=0.2,\beta=0.7$; (f) $\alpha=0.5,\beta=0.7$; (g) $\alpha=0.6,\beta=0.25$; and (h) $\alpha=0.6,\beta=0.1$.

lyzed. The parameters are the same as in Sec. II. In Fig. 2, the phase diagram is plotted, which consists of four regions. In the free flow phase, the system is jam-free [Fig. 3(a)]. Hence the current is determined by the inflow parameter α. In the plot of current vs bulk density (Fig. 1), the data of free flow phase collapse into the monotonous increasing part of the upper branch of the fundamental diagram.

In the congested phase I, the system is a coexistence of jams, free flow, and synchronized flow [Fig. 3(b)]. Due to the hindrance of the right boundary, the synchronized flow occurs upstream of the boundary. Since the synchronized flow is not stable, the jams are self-organized from the synchronized flow. The jams propagate upstream, and downstream of it the free flow occurs. As β increases, the jams are more easily self-organized. Consequently, the region of synchronized flow in the space-time plot shrinks [Fig. 3(c)]. When β decreases, the self-organization of the jams is more difficult. As a result, the region of synchronized flow expands [Fig. 3(d)].

When β is quite large, the synchronized flow can only be maintained near the right boundary and the space-time plot in the bulk is characterized by the striped structure, i.e., jams alternating with free flow regions [Figs. 3(e) and 3(f)]. For the case, when the jam arrives near the left boundary and is

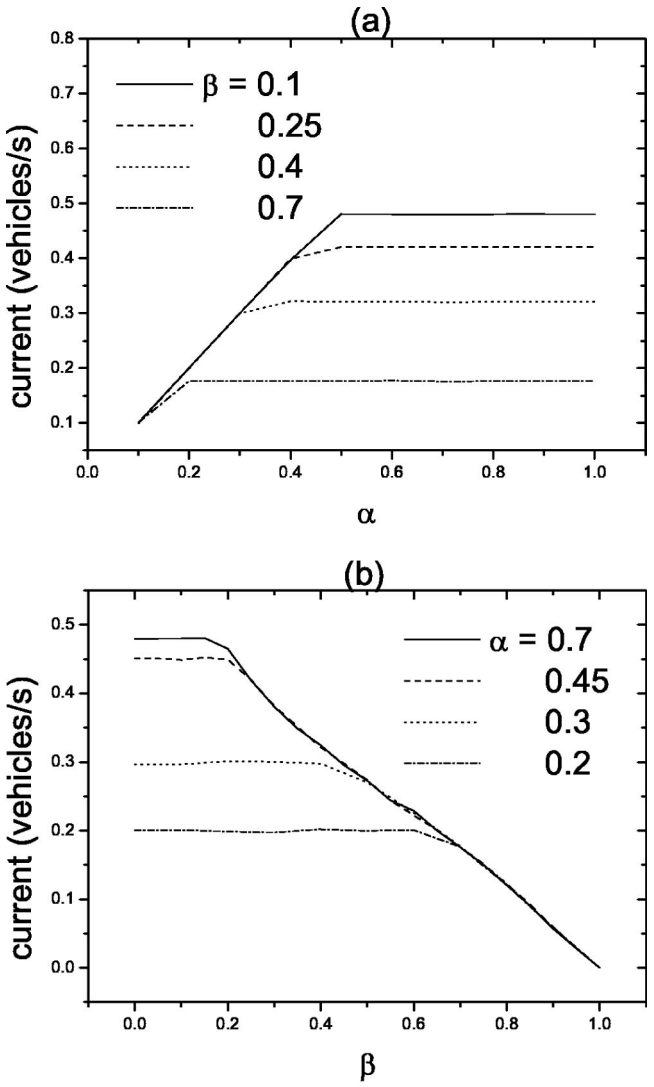

FIG. 4. The dependence of the current q on the parameters α and β.

exposed to the entrance flux, two subcases can be classified: when $\alpha<\alpha_c\approx 0.38$, the width of the jam decreases in average because the inflow is smaller than the outflow of a jam [Fig. 3(e)]; when $\alpha>\alpha_c$, the width increases in average [Fig. 3(f)]. These two subcases are similar to the phases of jams I and II in the VDR model, one kind of the STS models, except near the right boundary (see Fig. 8 in Ref. [17]).

In the plot of current vs bulk density, the data of congested phase I collapse into the lower branch of the fundamental diagram when β is large, and they connect the upper branch and the lower branch of the fundamental diagram when β is small.

When $\beta_1<\beta<\beta_2$, one can have the congested phase II. For the case, the synchronized flow is stable and no jam will appear [Fig. 3(g)]. Thus, it is named synchronized flow (SF) phase. The SF phase corresponds to the synchronized flow pattern as observed by Kerner [21], where no wide moving jams emerge. In the plot of current vs bulk density, the data of SF phase collapse into the monotonous decreasing part of the upper branch of the fundamental diagram.

Finally, if $\beta<\beta_1$ and $\alpha>\alpha_1$, the maximum current (MC) phase is observed [Fig. 3(h)]. In the MC phase, the flow is not restricted by the boundaries but rather by the maxiumum possible bulk flow of the given model. In the plot of current vs bulk density, the data of MC phase collapse into a point.

Now one can see that the lower branch of the fundamental diagram in the PBC is classified into two ranges. The large density range can be generated in the OBC while the small density range cannot be generated. This means not all the possible bulk states are generated by the chosen open boundary conditions. This phenomenon is also reproduced and explained in the work of Namazi *et al.* [22], where the car-following model is used.

We compare our phase diagram with that of VDR model (see Fig. 8 in Ref. [17]). It can be seen that our phase diagram is quite different: the MC phase appears but the JO phase disappears. Moreover, the congested phases of the MCD model (including congested phase I and SF phase) are quite different from those of the VDR model (including jams I and II) despite the similarity at large β. These differences are obviously caused by the nonmonotonicity of the MCD model.

We would like to mention the implications of our results for real traffic. That is, for a road section, if there is no hindrance at the downstream end (i.e, $\beta=0$), then the jam will never occur. Thus, in order to prevent the appearance of jams, particular attention should be paid to the downstream end of the road section rather than to the entrance. From the viewpoint of whole road networks, a hindrance at the downstream end of each section corresponds to a bottleneck, so particular attention should be paid to reducing bottlenecks.

Next we investigate the current in the OBC. In Fig. 4, we show the dependence of the current q on the parameters α and β. In Fig. 4(a), β is fixed and the curves of q against α are plotted. One can see that in the free flow phase, the current increases with the increase of α while it remains constant in other phases. In Fig. 4(b), α is fixed and the curves of q against β are plotted. One can see that in the free flow phase and in the MC phase, the current remains constant while it decreases with the increase of β in other phases.

IV. DENSITY PROFILE

In this section we focus on the density profiles. Since a vehicle has a length of five cells, the density is defined as the average density in every five cells.

In the free flow phase, when α is relatively large, the profile is flat in the bulk [Figs. 5(a) and 5(b)]. Near the left end, a fluctuation is observed.[3] The fluctuation is smeared out due to the randomization. We denote l as the distance within which the density reaches the asymptotic value. As α

[3]The study on density profile in OBC starts from the ASEP. Later it is extended to traffic flow models with $v_{max}>1$. The density defined in this study is somewhat different from the classical density: it denotes the cell occupation. Thus, an oscillated profile in Fig. 5 does not imply an inhomogeneous traffic.

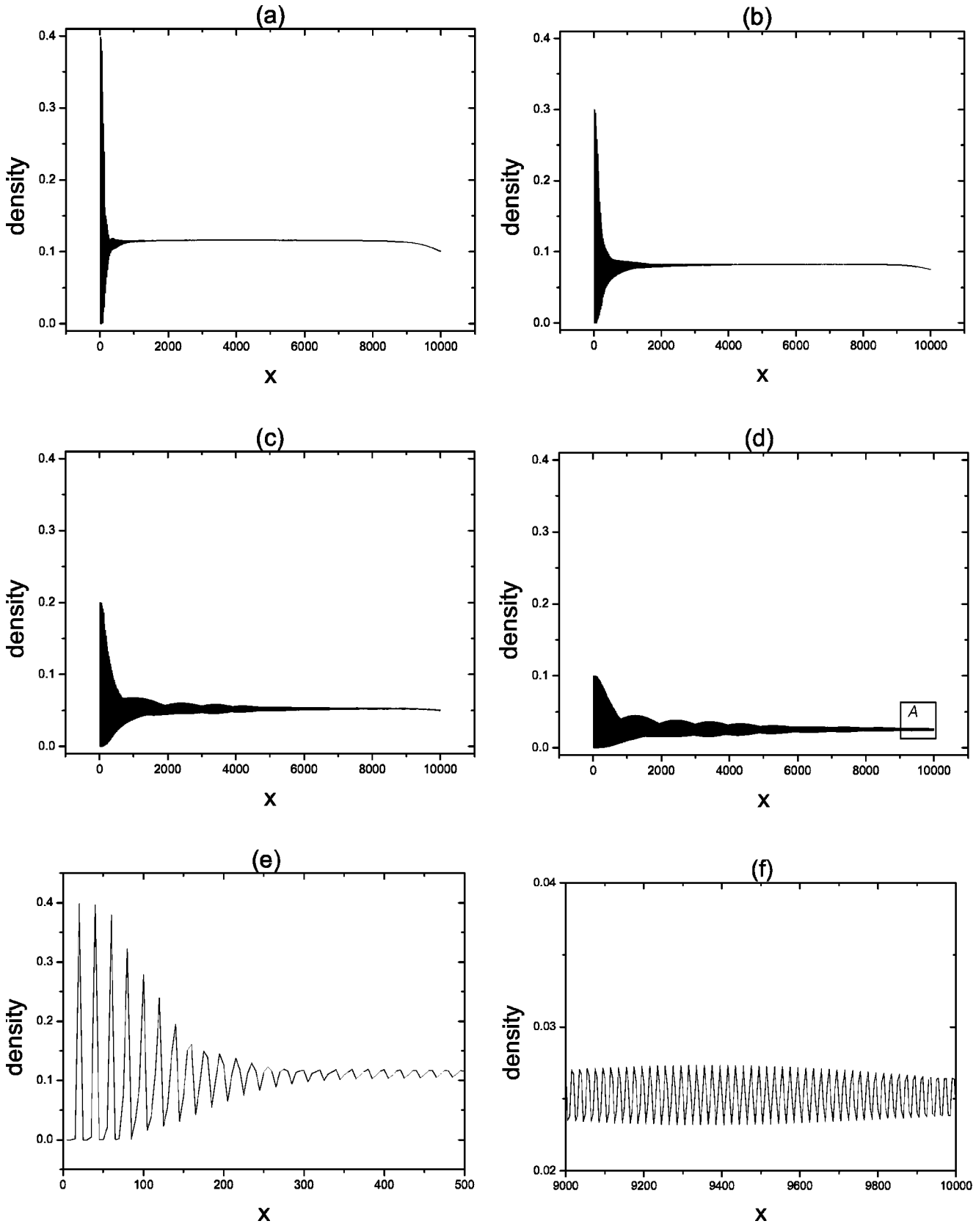

FIG. 5. The density profiles in the free flow phase. (e) gives the details of (a) near the left boundary and (f) gives the details of inset *A* in (d). $\beta=0$. In (a) $\alpha=0.4$, (b) $\alpha=0.3$, (c) $\alpha=0.2$, and (d) $\alpha=0.1$.

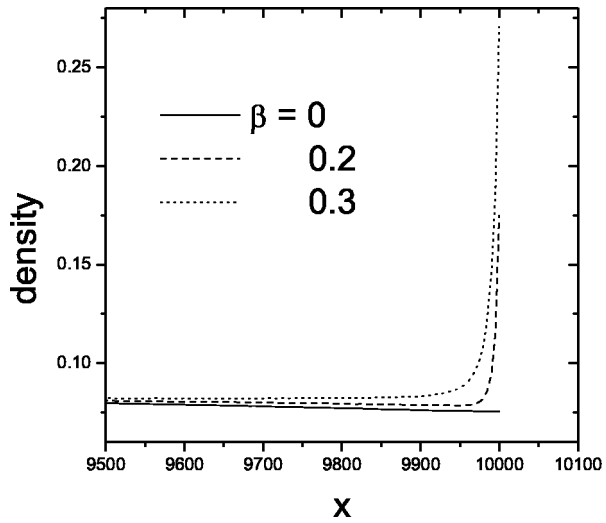

FIG. 6. The density profiles in the free flow phase near the right boundary with α fixed at 0.3.

decreases, the bulk density as well as the maximum value of the amplitude of the oscillation decreases, but l increases [Figs. 5(a)–5(c)]. The oscillating profile finally occupies the whole system [Fig. 5(d).

Near the left end and in the bulk, the densities are independent of β, the influence of β can only be observed near the right end. In Fig. 6, we show the density profiles near the right end with α fixed at 0.3. It can be seen that for $\beta=0$, the densities decay near the right end. With the increase of β, the decay becomes weaker and an increase of the density at the end of the system occurs ($\beta=0.2$). When β is larger, the decay vanishes and the densities increase monotonically as one approaches the right end ($\beta=0.3$).

Our results are different from that in Ref. [16], where the densities always increase smoothly up to the site $L-1$ and a sudden drop of density is observed on the last site.[4] This is due to the fact that the right boundary condition used in Ref. [16] is different. In Ref. [16], the right boundary is fulfilled by sitting a stationary car at the site $L+1$ and vehicles are removed with a given probability provided the last site is occupied. As a result, a vehicle needs to decelerate when approaching the right boundary even if the removal probability is 1.

In the congested phase I, when β is large, a flat profile is observed in the bulk, which corresponds to the striped structure. However, since the synchronized flow is maintained near the right boundary, the density increases monotonically as one approaches the right end (Fig. 7, $\beta=0.8$). As β decreases, the region of synchronized flow expands. As a result, the flat profile in the bulk shrinks ($\beta=0.7$). When $\beta=0.6$, the flat profile disappears.

If one continues decreasing β, the profile gradually tends to flatness again. In addition, we note that an increase of the density at the end of the system occurs and enhances with the decrease of β.

[4]Note that each cell corresponds to 7.5 m and a vehicle has a length of one cell in Ref. [16]

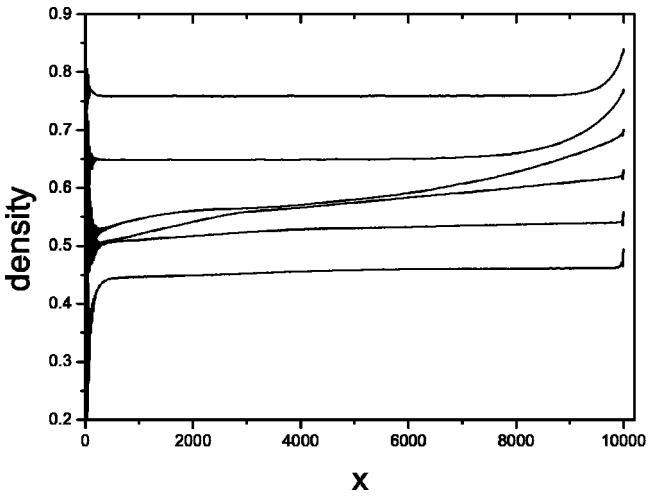

FIG. 7. The density profiles in the congested phase I. $\alpha=0.4$; $\beta=0.8,0.7,0.6,0.5,0.4,0.32$ from top to bottom.

The density profile in the congested phase I is different from those in the congested phase in NS and VDR models [15,16], where only flat profile exists in the bulk. This is caused by the coexistence of the three phases: jam, free flow, and synchronized flow in MCD model.

In the SF phase, there is no jam and the profile remains flat in the bulk (Fig. 8). An increase of the density always exists at the end of the system. When β decreases, the flat profile in the bulk assumes a lower value and the increase of the density at the end of the system enhances.

The influence of α can only be observed near the left end in both congested phase I and SF phase (Fig. 9). With the decrease of β, the region affected by α first expands and then shrinks: it reaches the widest at $\beta\approx0.5$. Moreover, the fluctuation of the density profile near the left end also exists in the congested phase I and SF phase. With the increase of α, the fluctuation becomes weaker.

In the MC phase, the simulations show that the profile is a monotonous decreasing function in the bulk, which does not depend on α and β (Fig. 10). The influence of $\alpha(\beta)$ can

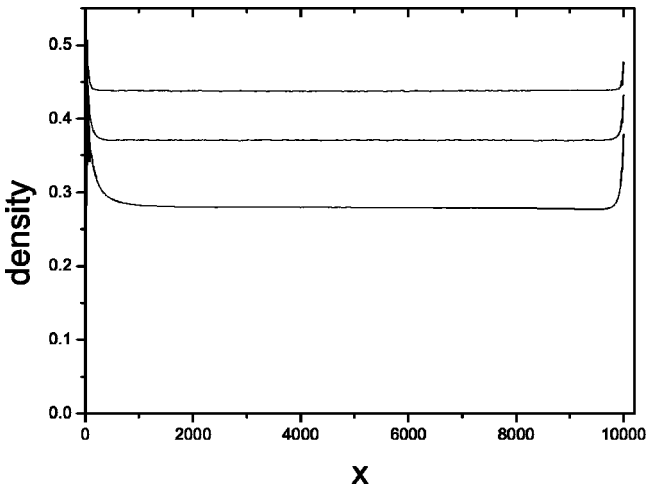

FIG. 8. The density profiles in the SF phase. $\alpha=0.6$, $\beta=0.3,0.25,0.2$ from top to bottom.

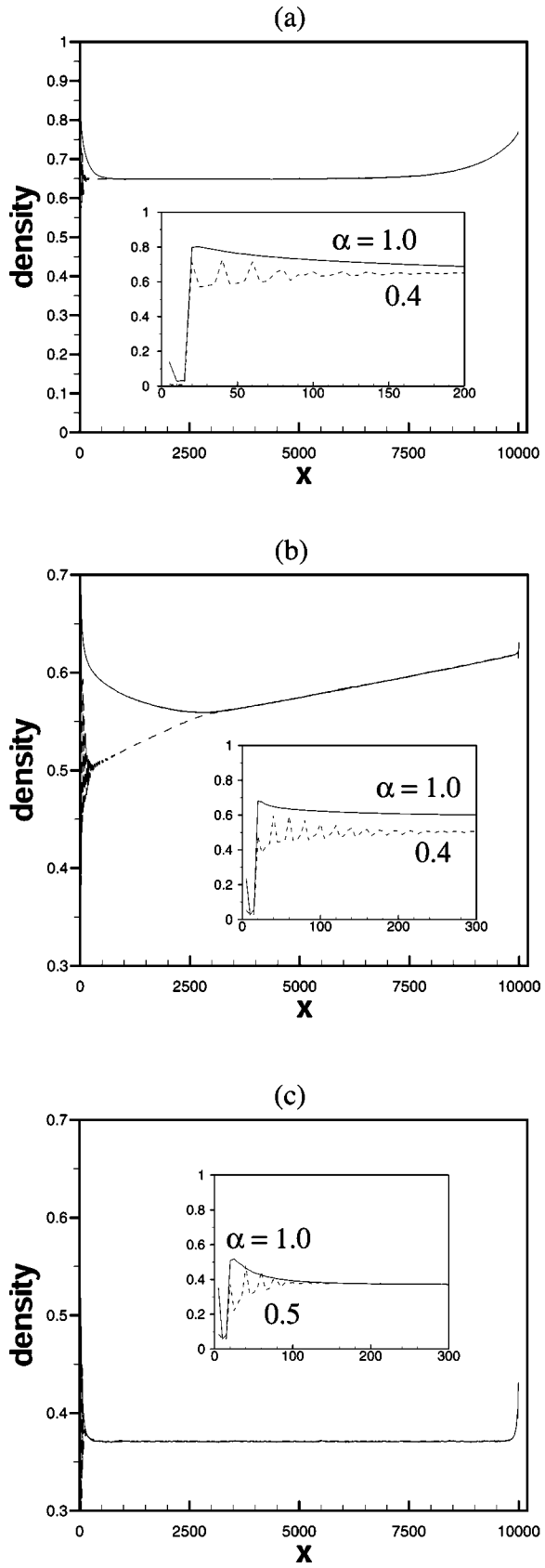

FIG. 9. (a, b) The density profiles in the congested phase I and (c) in SF phase. In (a) $\beta=0.7$, (b) $\beta=0.5$, and (c) $\beta=0.25$. The inset gives the details near the left boundary.

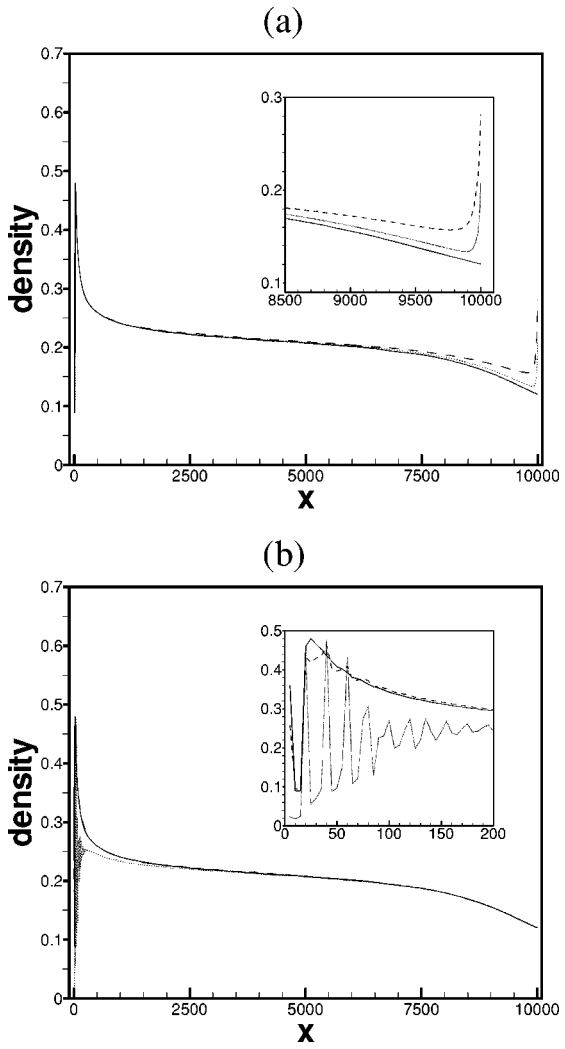

FIG. 10. The density profiles in the MC phase. In (a) $\alpha=1.0$, the solid line, dotted line, and dashed line correspond to $\beta=0,0.1,0.15$. In (b) $\beta=0$; the solid line, dashed line, and dotted line correspond to $\alpha=1.0,0.8,0.5$. The inset gives the details near the right boundary in (a) and left boundary in (b).

only be observed near the left (right) end. For $\beta=0$, the density decays near the right boundary. With the increase of β, the decay becomes weaker and an increase of the density at the end of the system occurs and enhances [Fig. 10(a)]. This is similar to that in the free flow phase. At the left boundary, the fluctuation of the density profile still exists and it weakens with the increase of α [Fig. 10(b)]. This is similar to that in the congested phases.

V. CONCLUSIONS

In this paper, we have discussed the traffic situations of the MCD model in the OBC. This model exhibits the metastable states and the hysteresis in the PBC. Nevertheless, different from the STS model, the upper branch of the fundamental diagram of the model is not monotonous but has an extremum.

The phase diagram of the model in the OBC is investigated, which consists of four phases. The typical space-time

plots of the four phases are given. Compared with that of the VDR model, the new phase MC appears but the phase JO disappears. Apart from this, the congested phases of the MCD model are quite different from those of the VDR model.

The fundamental diagram in the OBC is studied and compared with that in the PBC. It is shown that the data of different phases collapse into different parts of the fundamental diagram. We find that the branched fundamental diagram in the PBC turns into a nonbranched one in the OBC.

The dependence of the current q on the parameters α and β is discussed. The simulations show that when β is given, the current increases with the increase of α in the free flow phase while it remains constant in other phases. On the other hand, when α is fixed, the current remains constant in the free flow phase and in the MC phase while it decreases with the increase of β in other phases.

The density profiles in the OBC are also investigated. It is shown that in different phases, the profile is qualitatively different. We find that except near the boundaries, the profile is flat in the free flow phase (when α is not small) and SF phase but is monotonically decreasing in MC phase. In the free flow, the oscillating profile may occupy the whole system if α is small. In the congested phase I, the profile may not be flat in the bulk due to the coexistence of jams, free flow, and synchronized flow.

ACKNOWLEDGMENT

We acknowledge the support from the National Natural Science Foundation in China (NNSFC) with Grant No. 10272101.

[1] *Traffic and Granular Flow '97*, edited by M. Schreckenberg and D.E. Wolf (Springer, Singapore, 1998); *Traffic and Granular Flow '99*, edited by D. Helbing, H.J. Herrmann, M. Schreckenberg, and D.E. Wolf (Springer, Berlin, 2000).
[2] D. Chowdhury, L. Santen, and A. Schadschneider, Phys. Rep. **329**, 199 (2000).
[3] D. Helbing, Rev. Mod. Phys. **73**, 1067 (2001).
[4] M. Bando *et al.*, Phys. Rev. E **51**, 1035 (1995); D. Helbing and B. Tilch, *ibid.* **58**, 133 (1998); R. Jiang, Q.S. Wu, and Z.J. Zhu, *ibid.* **64**, 017101 (2001); M. Treiber, A. Hennecke, and D. Helbing, *ibid.* **62**, 1805 (2000); E. Tomer, L. Safonov, and S. Havlin, Phys. Rev. Lett. **84**, 382 (2000).
[5] K. Nagel and M. Schreckenberg, J. Phys. I **2**, 2221 (1992).
[6] S.C. Benjamin, N.F. Johnson, and P.M. Hui, J. Phys. A **29**, 3119 (1996); R. Barlovic *et al.*, Eur. Phys. J. B **5**, 793 (1998).
[7] D. Helbing *et al.*, Transp. Res., Part B: Methodol. **35**, 183 (2001).
[8] M.J. Lighthill and G.B. Whitham, Proc. R. Soc. London, Ser. A **229**, 317 (1955).
[9] H.J. Payne, in *Mathematical Models of Public Systems*, edited by G.A. Bekey (Simulation Council, La Jolla, 1971), Vol. 1.
[10] A. Aw and M. Rascle, SIAM (Soc. Ind. Appl. Math.) J. Appl. Math. **60**, 916 (2000).
[11] R. Jiang, Q.S. Wu, and Z.J. Zhu, Chin. Sci. Bull. **46**, 345 (2001); Transp. Res., Part B: Methodol. **36**, 405 (2002).
[12] H.Y. Lee, H.W. Lee, and D. Kim, Phys. Rev. Lett. **81**, 1130 (1998); Phys. Rev. E **59**, 5101 (1999).
[13] S. Wolfram, *Theory and Applications of Cellular Automata* (World Scientific, Singapore, 1986).
[14] A.B. Kolomeisky *et al.*, J. Phys. A **31**, 6911 (1998).
[15] S. Cheybani, J. Kertesz, and M. Schreckenberg, Phys. Rev. E **63**, 016108 (2001).
[16] D.W. Huang, Phys. Rev. E **64**, 036108 (2001).
[17] R. Barlovic *et al.*, Phys. Rev. E **66**, 046113 (2002).
[18] C. Appert and L. Santen, Phys. Rev. Lett. **86**, 2498 (2001).
[19] R. Jiang and Q.S. Wu, J. Phys. A **36**, 381 (2003).
[20] W. Knospe *et al.*, J. Phys. A **33**, L477 (2000); Phys. Rev. E **65**, 015101 (2002).
[21] B.S. Kerner, Phys. Rev. E **65**, 046138 (2002).
[22] A. Namazi *et al.*, Eur. Phys. J. B **30**, 559 (2002).